ANNALS of Faculty Engineering Hunedoara
– International Journal of Engineering
Tome XIV [2016] – Fascicule 3 [August]
ISSN: 1584-2665 [print; online]
ISSN: 1584-2673 [CD-Rom; online]
a free-access multidisciplinary publication
of the Faculty of Engineering Hunedoara

[1.]Antoni JOHN, [2.]Grzegorz KOKOT

EXPERIMENTAL TESTING AND NUMERICAL SIMULATION OF BONE TISSUE

[1-2.] Silesian University of Technology, Gliwice, POLAND

ABSTRACT: In this paper the selected problems of modeling human biomechanical structures are presented. One of the biggest problems in investigation of bioengineering is the determination of the material properties of anatomical structure, i.e. for cancellous and cortical bone. The main obstacle which came across is the lack of possibility to conduct the quantitative computed tomography (QCT). The simplification from heterogeneous orthotropic model of bone's material to homogeneous isotropic material is too high for the proper accurate evaluation of stress and strain state and compliance of bone. Experimental and numerical determinations of material parameters of bone tissue are presented. Finally, selected complex problems concern biomechanical structures were solved using FEM.
Keywords: experimental testing, Digital Image Correlation method, computed tomography, FEM

1. INTRODUCTION

Nowadays a sedentary way of life is amplified by poor quality of food and watching television instead of doing any sport etc. This conditions are leading to bad state of human body already in early time of life. It may lead to damage of such parts of human body like joints rather in normal condition of functionality, not only in high overloaded states. The reason for such state it could be weakening of bone, cartilage and synovial liquid.

Advanced FE systems make it possible to prepare a numerical model of complex biomechanical structures - especially with respect to joints in human locomotion system. It is particular important when the THA operation is performed and the artificial acetabulum is fitted. Very often before and after operations the knowledge of the stress and strain distribution in the pelvic joint (pelvic bone and femur) is needed.

The process of modelling is one of the most important steps of this research. The precision of preparing the model influences meaningfully the precision of the results and time of solving the task by computer system and it could be divided into:

1. Preliminary preparation of geometry based on filtered CT scan data.
2. Division model to finite elements.
3. Assignment of material data.
4. Assignment of boundary condition and analysis.

The first part of our investigation concern determination of material parameters of bone tissue in experiment and the second part concern the numerical simulation of selected problems in human joints.

2. DETERMINATION OF MATERIAL PARAMETERS

The basis for testing of bone elastic properties (Young and Kirchhoff modulus, Poisson ratio) is a known mechanical tests like tension or compression, where during the cross head movement the force-displacement curve is registered. The important thing is the displacement measurement.

The simplest measurement is provided by the testing machine, the so-called measurement of the cross head movement. However, it is characterized by rather large inaccuracy in the case of bone tissue. A significant improvement is achieved by the use of extensometers, however, due to the porous structure of the material and the small size of samples their application is also limited. Better results of the research provide optical methods, such as holographic interferometry and speckle photography. They provide non-contact measurement what is a significant advantage in the study of the bone structure. Although these methods have limitations associated with the registration of measurement (spot measurement, poor camera, no extensive software, poor digitization process), their use greatly expanded the accuracy and quality of the measurements.
Currently being developed optical methods of measurement of displacements and deformations, using advances in recording and processing of digital images, provide an online view of the field of displacements and deformations of the tested structure. Computer aided measurement allows to record and observe phenomena such as the concentration of deformation or crack formation and propagation.
This article presents the classic measurement methods with particular emphasis on their application in the study of bone, taking into account the methods for measuring displacement and selection of samples for testing.

2.1. Compression test

One of the base test is tension or compression test. As most of the human skeleton parts work in compression condition the compression test is the mostly used test in bone tissue testing. The test is directly taken from experimental mechanics where sample is putted between two stiff platens and is compress with applied load. The typical testing stand is presented on the Fig. 1a and tested samples on the Fig. 1b and 1c.

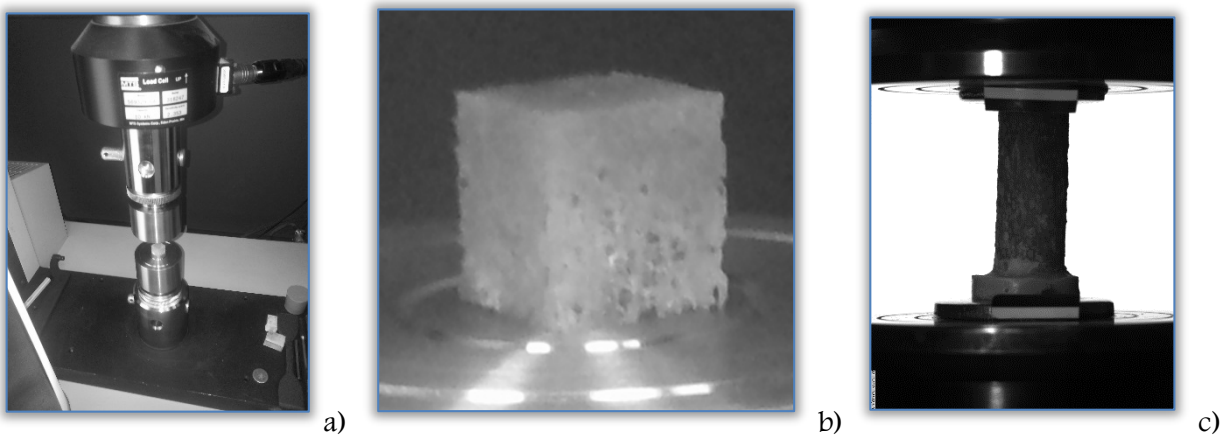

a) b) c)

Figure 1: Compression platens (a), the cubic specimen (b) and cylinder specimens (c)

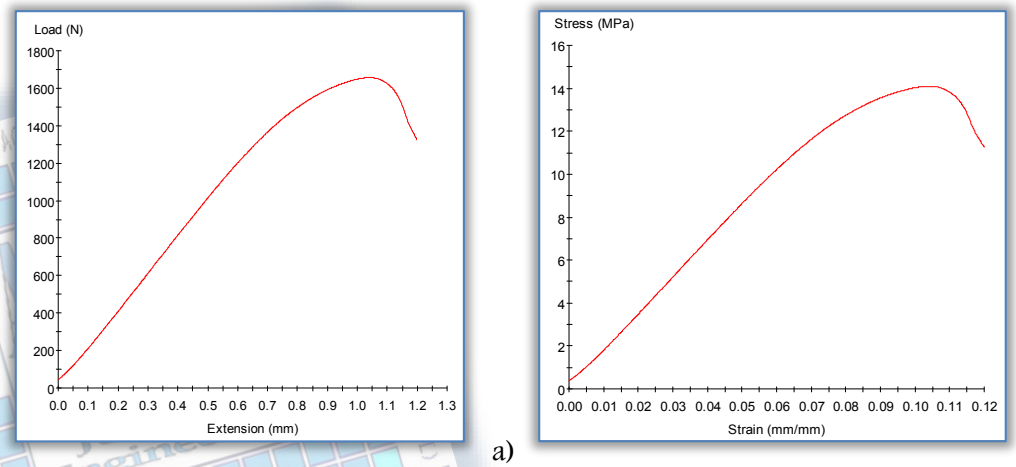

a) b)

Figure 2: Typical compression load-extension (a) and stress-strain curve (b) for the spongy bone

Due to the nature of the tested material the sample dimensions deviate from the recommendations of code for common materials. It is understood that the tensile test is carried out on samples of cylindrical or rectangular shapes and compression test on the cubic shape samples. Detailed discussion of sampling, dimensions and their impact on the results is presented in the papers [1], [2], [3].

The typical disadvantages are the sample mounting and displacement measurements. In the case of the cylindrical samples they are often planted in the resin. But the most serious difficulties are mostly connected with displacement measurement and low precision and accuracy of results. This is due to small specimen size, complicated mounting way and porous structure of the tested material, often additionally under wet condition. The other thing is the hierarchical structure of the bone which strongly influence on the mechanical properties on the macro- and micro level. Typical compression load-extension and stress-strain curve for the spongy bone are presented on the Fig. 2 (own research).

2.2. Three point bending

The second mostly used testing method of the cortical bone is tree or four point bending (Figure 3). The studies have been performed using human femora dissected from cadaver body from female donor 30 years old.. The specimens were dissected from femora diaphysis. The 4x4x40 mm cube shape size of each sample was mechanically machined. Each sample where measure by digital slide caliper (Mitutoyo, resolution 0.01 mm) to control the accuracy of the machining.

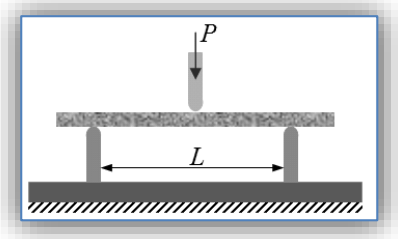

Figure 3: Scheme of the three point bending

Based on the curve of load-deflection of the beam and the theory of bending beams the mechanical properties are defined, among others, elastic modulus. For 11 samples obtained an average score of E = 14544 MPa with a standard deviation of 2470 MPa. The testing stand and sample are presented on Fig. 4.

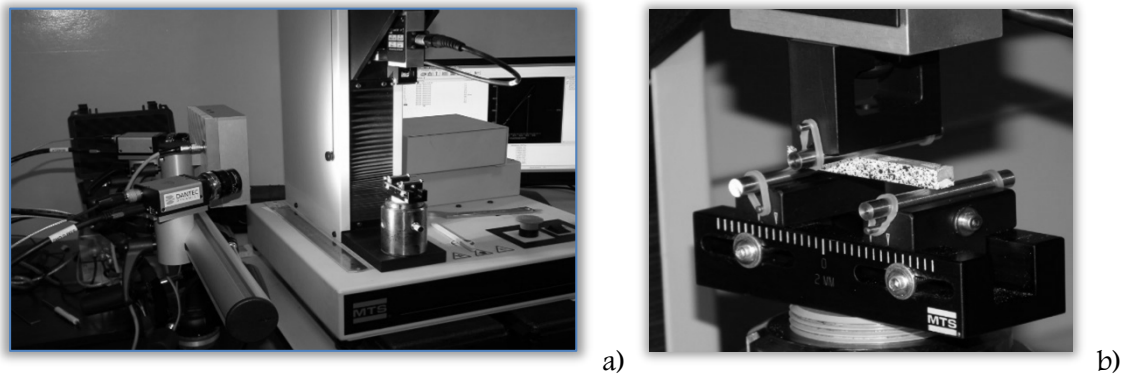

a) b)

Figure 4: Three point bending test: a) testing stand with DIC system, b) bending table with the specimen

Next, for the one specimen with Young modulus E≅22200 MPa and ultimate tensile strength S=319 MPa with max. deflection y=0.69 mm the numerical simulation was performed. The sample was scanned by X-ray microcomputed tomography (XMT) scanner (Nikon Metrology, X-tek, Tring, UK). Scanning settings (kV, μA, no filter, 2000 projections, voxel size 20 μm) were adjusted using the manufacturer software. The density phantom was scanned together with the specimen to enable quantitative measurement of the bone mineral density. After image acquisition reconstruction of cross-sectional axial images were performed. The total volume of interest contains 2000x2000x2000 voxels from about 356 000 voxels were busy with the bone friction. The reconstructed volume was stored in the single file (32-bits real, little endian) on the computer hard drive. The FE model with material parameters was generated automatically, based on approach described by [4] and own developed software [5]. For each voxel contained bone one element (HEXA 8-noded) was defined. Based on calibrated grey value material parameters (Young modulus *E*, ultimate strength *S*) have been defined. Relationship which connects calibrated bone density with material properties were defined based on following equations:

$$E = 10.5 + 0.0102\rho_{QCT}; \quad (1)$$

$$S = 63.8 + 0.184\rho_{QCT} \quad (2)$$

-where ρ_{QCT} – density calibrated based on greyscale and calibration curve.

This gives the model with non-homogenous material parameters what is closer to the reality then taking into account the model with one material with linear properties. The FE model was built using the HEXA 8-noded elements and consist of about 3 mln DOF. Specimen with material parameters is presented on Figure 5a. Boundary condition were taken from the experiment and modelled in the MSC.Patran (Figure 5b). Simulation were performed using the MSC.Nastran

solver. The results from simulation matched the results from the experiment. The numerical calculations using finite element method give the deflection and stresses comparable with experimental results. It shows that the numerical analysis of models generated on the base of X-ray microcomputed tomography (XMT) scans with material parameters described based on Hounsfiled scale can be used as the tool for determining the mechanical properties of bone. The computational methods primary used in mechanics can be useful for solving the biomechanics problems too.

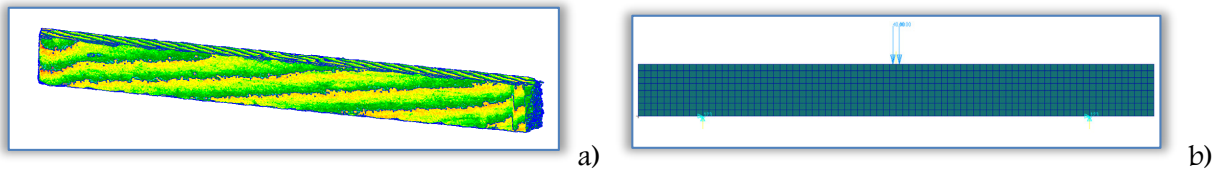

a) b)

Figure 5. The specimen FE: a) model generated from XMT with assigned materials properties, b) FE model with boundary conditions

2.3. Digital Image Correlation

The Digital Image Correlation is an optical full-field technique for non-contact, 3D deformation measurements, where the high contrast speckle pattern applied onto the surface of the sample is observed by the CCD cameras during loading (Figure 6). Specialized software is used to analyzing the captured images during deformation and recalculation them to the form of the displacements/strains field (Figure 7) which can be directly compare with results from the FE analysis. This is the great opportunity to direct validation of the numerical models.

In the conducted research the DIC system was combined with the classical experimental tests (tension/compression, three point bending). Such combination considerably enhances possibility in evaluating the mechanical properties of bone tissues, particularly at the macrostructure level.

Figure 6: The testing stand with the Digital Image Correlation

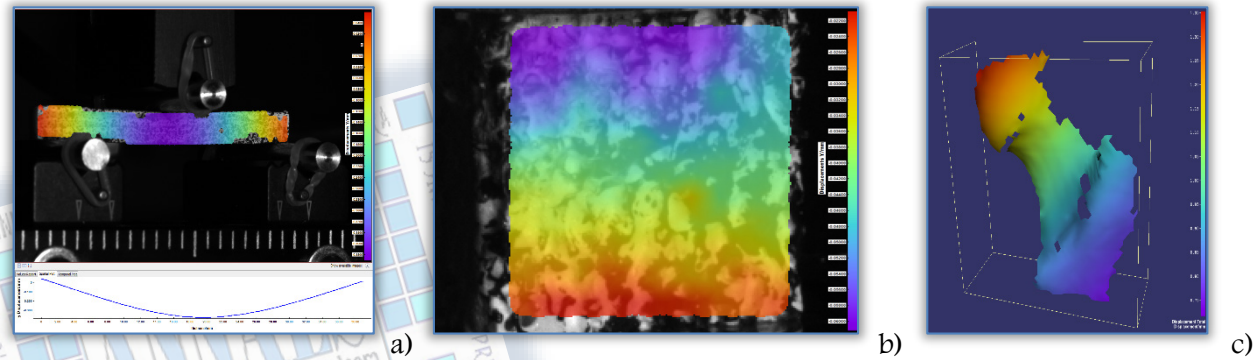

a) b) c)

Figure 7: Sample results using DIC for three point bending (a), compression test (b) and macro testing of the femur (c)

2.4. Nanoindentation

This is relatively new method in the experimental mechanics for testing the hardness and Young modulus. Main advantage is the measurement on the micro- or even nanostructure level. Characteristic for this method is the penetration force range: from mili to microniutons.

The main idea for testing Young modulus is that the penetrator penetrate the sample with the specified force and then sample is controlled unloaded. The first part of unloading curve is connected with ideal elastic behavior of sample. On this basis the Olivier and Pharr developed the method for determining the Young modulus [6,7]. Tested parameters are calculated directly from the loading-unloading curve (Figure 8). Figure 9 presents the nanoindentation testing stand.

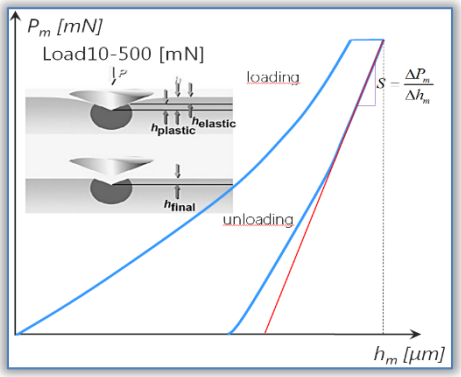

Figure 8: The nano-indentation curve

Very important in this technique is the proper setup of the testing parameters: load force and times of individual phases. On the base of the conducted series of tests for single trabecula (Figure 10) the Young modulus vary between 8.4-13.3 GPa, the Vicers micro-hardness vary between 50.1-55.9 (Table 1). The example of testing the cortical bone is presented on the Figure 11.

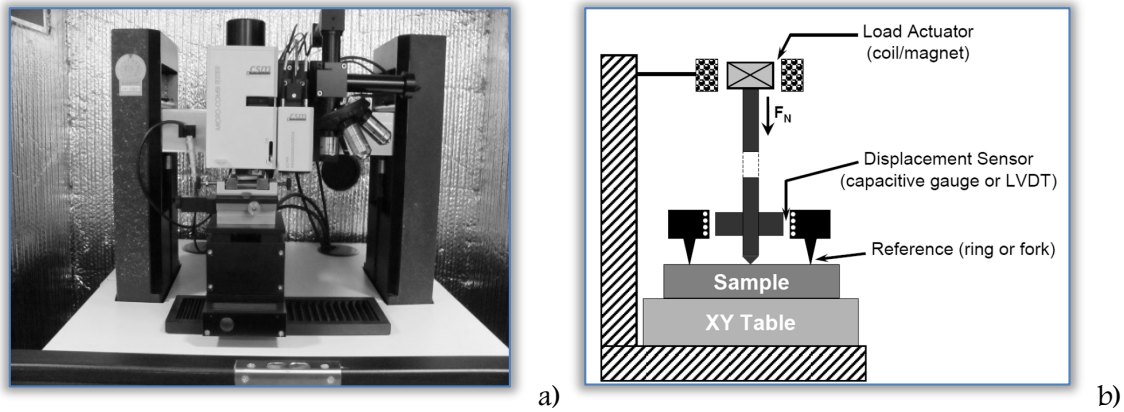

a) b)

Figure 9: The nano-indentation testing stand: a) real object (photo), b) schema

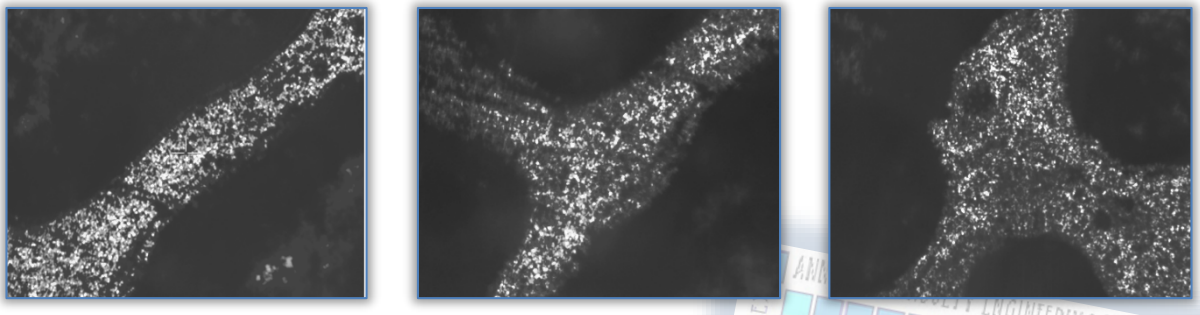

Figure 10: Single trabeculaes under microscope with measurement points

Table 1. Results of nanoindentation test of bone tissue

	test	F [mN]	E [GPa]	H_{IT} [MPa]	H_{VIC} Vickers
Trabeculae	1	200	8.494	500.3	47.2
	2	200	8.424	564.5	53.3
	3	200	8.299	545.8	51.5
	avg.		**8.4**	**536.9**	**50.7**
Node I	1	200	9.854	592.0	55.8
	2	200	10.324	542.0	54.4
	3	200	9.954	584.0	57.6
	avg.		**10.0**	**572.7**	**55.9**
Node II	1	200	13.664	514.3	48.5
	2	200	13.666	593.0	55.9
	3	200	12.635	485.5	45.8
	avg.		**13.3**	**530.9**	**50.1**

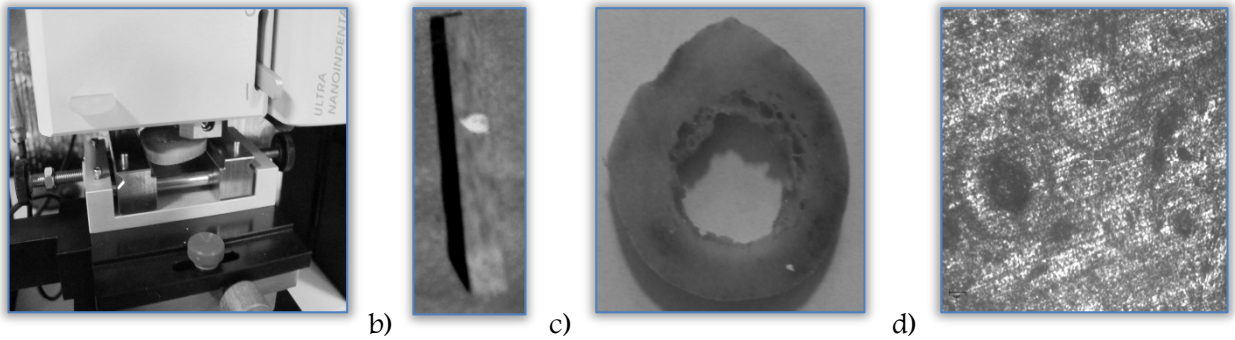

Figure 11: Nano-indentation: a) testing stand, b), c) samples, d) microscopic view of the tested places

3. NUMERICAL SIMULATIONS

3.1. Simulation of human gait for orthotropic model of pelvis-femur set

The way of creating numerical model was similar to the one presented in our previous work [8,9]. The models of bone specimens were created on the basis of CT scans, took with high accuracy (0.347mm). The elements representing the cartilage of femur head and pelvic acetabulum were created manually because of damage of specimens. After building and assembling the CAD models were divided into high value of finite elements. Preparing of the finite element model was the most time consuming stage. The parts of femur and cartilage on femur head as well as pelvis and cartilage on pelvis acetabulum have node connections. The cooperating surfaces representing hip joint are spherical surfaces with the same origin of coordinate system to get the possibility to simulate human's gait. The next step it was to assign material data to each element. The special equations were used at this step [10,11]. The equations for cancellous bone of femur sometimes described material characteristic for pelvis due to lack of appropriate data [11]. In this work authors decided to use expressions for lumbar spine instead of the femur's expression. The justification of this approach was found in trials by sampling specific equations to convert the Hounsfield's unit (HU) to properly values of elastic modulus. The expression for femur cortical bone was also used to describe the pelvis cortical bone for the same reason like previous. The Poisson's ratio modulus for all objects and mineral density, Young modulus of cartilage were obtained by comparison data from literature [12,13]. The final results are shown in Table 1.

The twenty three muscles' forces were applied to pelvis to mimic stance phase of human gait according to Thompson M.S work [14]. The stance phase was divided into five stages (Fig. 11a). The time of movement was established on 0.8s equal the 60% of all time gait phase and the range of motion on 40 degree, -10 degrees from frontal plane into direction of sagittal axis to 30 degrees in opposite direction. These parameters were determined by measurement. The body mass was amount to 75 kg. The force system corresponding to the weight of upper body part acting on pelvic bone was changed into the equivalent force system shown Fig. 11b. The quality of synovial liquid was simulated by different value of coefficient of friction between cooperating surfaces on cartilages equalling: 0.003, 0.01. The model of friction was the coulomb stick-slip model which could be chosen in MSC Marc software where analyses were conducted. The degrees of freedom were taken in vertical direction in pubic bone and in connection of pelvis bone with spine.

The concentration of stress (Huber-Misses hypothesis) and maximal principal strain on femoral neck could be noticed, what is consent with general distribution forces from upper part of body [6]. It could be reason to femoral neck brakes which are considered for orthopaedists to one of most dangerous, especially for older persons. This type of femur damage very often founds treatment in arthroplasty. The results could be discussed on pelvic acetabulum cartilage example.

The maximal principal strains were observed during 0-0.2s of total time of stance phase of gait which is the heel strike stage. The area of concentrations of strains could be observed in upper and frontal part of cartilage. It could be a result like a complex system of femur's motion and force from mass of upper part of body. In this same area the maximal stress were noticed. The stresses' area were occur in pelvis acetabulum during gait, with maximal value in second stage. This could lead to the faster uses and to damaging of pelvis bone. There were not observed any of stress and strains concentration on femur head. The influence of coefficient friction value was significance in strains and stress level. The better value for stress was 0.003, not 0.01 like it was suspected. The value of stress was the lowest in all stages with exceptions of foot flat stage. The level of maximal principal strains was higher for 0.003 coefficient in foot flat stage as well as in

stresses' case but also in midstance stage. The difference between coefficient of friction was observed in minimal principal strains. The lower values were for 0.003 in all stages.

Table 2. Example of results of converting CT data to obtain the value of Young and Kirchhoff modulus. The symbols CF, CP means cartilage on femur head and on pelvic acetabulum respectively. Symbols: HU – Hounsfield's units, E-Young modulus, ρ - density, G – Kirchhoff modulus. The index 1,2,3 below E means directions of axes: 1- medial/lateral (or radial), 2-anterior/posterior (or circumferential), 3-superior/inferior (or longitudinal)

		Mineral Density [kg/m³]	Young modulus [GPa]			Kirchhoff modulus [GPa]			Poisson ratio		
			E_1	E_2	E_3	G_{12}	G_{23}	G_{31}	ν_{12}	ν_{23}	ν_{31}
Pelvis Femur Cortical bone	Max.	2211.65	16.03	15.88	24.82	6.13	4.90	11.09	0.307	0.622	0.119
	Min.	611.15	1.24	1.49	2.41	0.48	0.46	1.08	0.307	0.622	0.119
Pelvis Cancellous bone	Max.	413.6	0.76	0.53	2.15	0.32	0.22	0.89	0.2	0.2	0.2
	Min.	108.1	0.07	0.05	0.35	0.03	0.02	0.15	0.2	0.2	0.2
Femur Cancellous bone	Max.	451.10	0.87	0.86	1.73	0.36	0.36	0.72	0.2	0.2	0.2
	Min.	184.35	0.07	0.09	0.214	0.03	0.03	0.11	0.2	0.2	0.2
CF		1000	1.5	1.5	1.5	-	-	-	0.32	0.32	0.32
CP		1000	1.5	1.5	1.5	-	-	-	0.32	0.32	0.32

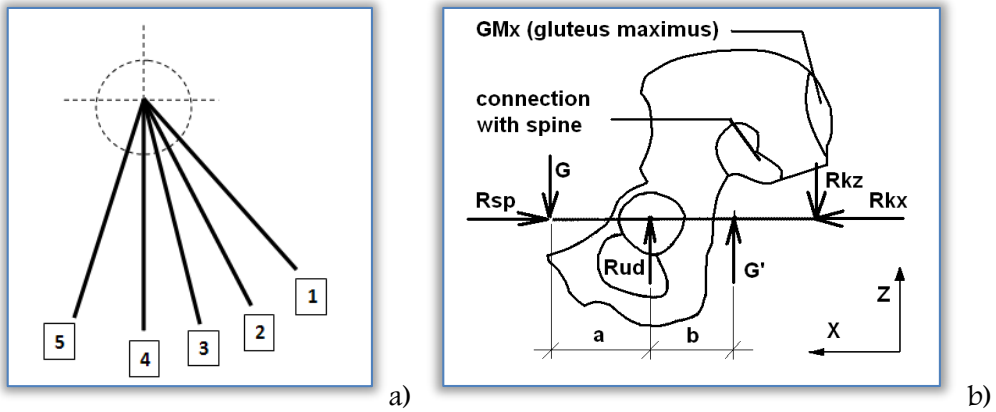

a) b)

Figure 12. Load system: a) stages of stance phase of human gait (1 - Heel strike, 2 - Foot Flat, 3 - Midstance, 4 - Heel off, 5 - Toe off), b) the equivalent force system (G – force from upper part of body, G' – equivalent force, G' = G(a/b), a = 30mm, b = 55mm, Rk – reaction of GMx, Rsp – reaction of right part of pelvis, Rud –reaction of femur)

The approach of complex boundary conditions and orthotropic materials' models in dynamic analysis of stance phase of human gait confirmed the predictions shown in the previous work [8,9]. The influence of coefficient friction on work in human hip joint could be noticed on basis of provided data from analyses. All research will be repeated for hip joint after arthroplasty and compare with conducted investigation in nearly future. It is very important to investigate which parts of femur and pelvis are the most loaded. This information could be very useful to design the prosthesis which will be able to transfer stresses and strains not exposing to damage the hip joint after arthroplasty.

3.2. Computer aided diagnostic of risky states in human bone system

Recognizing of dangerous state in human bone system can lead to prevent many defections. In this paper one concentrated on disorders in bones caused by osteoporosis. This is a systemic disease of skeleton which causes progressive decreasing of bone mass and changes in bone structure. In the course of time these changes are so serious that bones become weaker and weaker and can undergo accidental fractures. It is very difficult to diagnose this disease because it progress without symptoms: the first signs – difficulties during move and appearing pains in the spine and in the hip joint appear when it is the big loss of bone mass and it is the large risk of fractures. Unfortunately, it is a serious phase and the fractures are common – after fracture one should stabilization of places of fracture. There are many methods to detect osteoporosis. The large meaning have: Dual-energy X-ray absorptiometry (DXA) and Quantitative Computed Tomography (QCT). These methods lie in the phenomenon weakness of the radiation during crossing by through object. In the course of examination the part of radiation is absorbed or

distracted. The intensity of radiation depends on thickness and the content of minerals in the bone. In result of iterative reading of photos for individual pixels, the measurement density of whole object is obtained (exact to one pixel) [15-18].

Here, the QCT was used. Differences between healthy and osteoporotical state manifested in a little darker in CT slide 1. In this method the tomograms from CT are used to analyze the mineral density of bone. Through using the composition of projection images from different directions one can get cross-sectional and solid images in all researched structures. Tomograms consist of individual voxels. Each voxel is characterized by coordinates x, y, z and colour in gray scale. On the base of amount of radiation (absorbed in different places) one can determined density in these places with exact to one voxel. QCT differs than standard approach occurrence of density phantom which is X-rayed together with patients. The phantom is composed of regions representing specimens of bone density in Hounsfield Units. Here phantom consist in six specimens of bone. On the base of these standard density the calibration curve is drown. Exemplary of calibration curve is presented on Figure 13a. Formula of this curve enables to determinate the density for every voxel of researched bone. The density phantom is presented on Figure 13b. The images in QCT are created as a result of absorption the radiation through researched body. Because human tissues have different physical properties therefore coefficient of absorption has to also be different (it manifests various level of gray). By dint suitable software of tomographs computer and procedure of examination it is allowed to account the dose of absorbed radiation for each voxels [19]. The general course of QCT examination is following:

1. Performing of tomography researches. During examinations the bone system and density phantom is X-rayed. In a result the images (sections in different places) of analyzed object is received. The exemplary of tomograms of pelvic bone were presented in Figure 13c.
2. Analyzing the X-ray photographs by use specialist software (the dependence between quantity of the absorbed radiation and the radiological density in bone tissue is used).
3. Standardizing obtained density to Hounsfield scale – HU.

$$1HU = K\frac{\mu_p - \mu_u}{\mu_u} \tag{3}$$

where: K – amplification factor of images, μ_p – absorption factor, μ_u – absorption factor of reference object.

4. On the base of HU density determining the density of bone tissue.

$$\rho = 1.122 \cdot HU + 47 \tag{4}$$

5. Delimitation the material properties of bone tissue, especially elastic modulus (on the basis of experimental research the dependences between bone density and material properties were developed) [20,21].

$$E = 1.92\rho - 170 \tag{5}$$

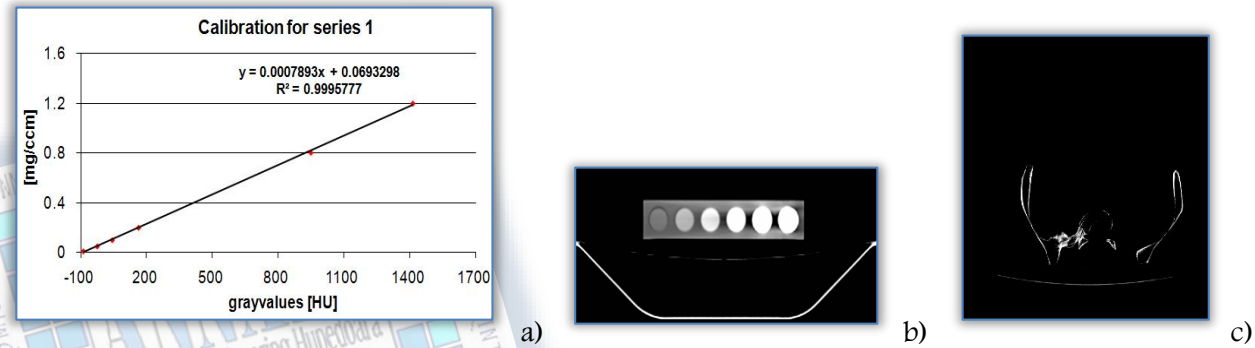

a) b) c)

Figure 13. Calibration curve (a) and exemplary images of pelvic bone from QCT: phantom (b), pelvic bone (c)

For the purpose of assignation material parameters obtained from QCT to numerical model the in-house procedure was used. On the base of QCT images (with resolution 512x512) the matrixes were get. Elements of these matrixes (with size 512x512) are material parameters determinated on the base gray scale. Next step is to combine all of these tables to one big matrix – 3D matrix. Additionally the text files with coordinates of nodes of our model were created: x.txt, y.txt, z.txt ([22,23]).

Algorithm of the program (Figure 14):

a. Creation of 3D table: [u, v, w] on the base of file combined.txt: coordinate u represents coordinate x, v represents z and w represents y in numerical model.
b. Modification of input file to MSC.Nastran: insertion value of elastic modulus on the base tomography to numerical model. In this way come into being FEM model in which in every finite element the individual material parameters were subortinated.

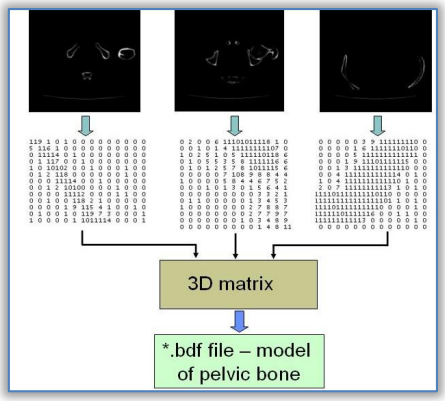

Figure 14. Procedure to converting images from QCT to create numerical model

The geometry was created on the base of date from QCT. The linear-elastic material was assumed. In modeled structure are three main parts:

» human pelvic bone (cancellous and cortical bone),
» endoprosthesis of hip joint (cement layer and artificial acetabulum),
» femur head (metal or ceramic).

The components of the model are presented in Figure15. In calculations the ideal joint between parts of model was accepted.

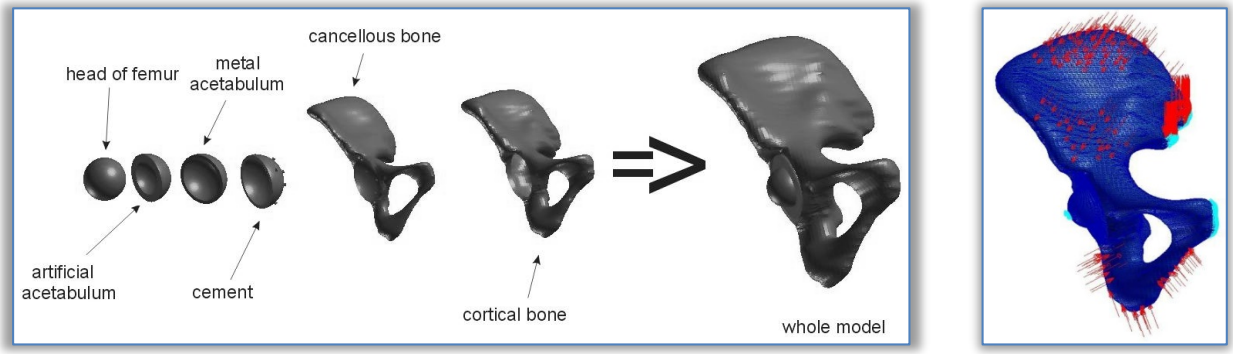

Figure 15. The components of model and model with boundary conditions

In the modeled object the following boundary conditions were assumed:

» fixed bearing in head of femur,
» roller support (displacement in vertical axis) in joint between pelvic and sacral bone and in pubic symphysis,
» nodal forces, which symbolize working muscular actons.

Strength calculations on the base FEM by system MSC Patran/Nastran/Marc were performed. Changes in human pelvic bone during progress of osteoporosis were considered as establishing material properties estimated on the base of QCT.

In a view of difficulties and limited access to images from tomography the numerical models were created also in different methods. Second approach consist of division all model to subregions – groups. Cortical bone was divided into five subregions, in each subregions elastic modulus is in the some range of value. The subregions of cortical bone consist of:

» pubic symphysis and joint of pelvic and sacral bone: 15000 –15600 MPa,
» surroundings of acetabulum: 13000–13500 MPa,
» upper part of ilium ala: 12000–12600 MPa,
» central part of ilium ala: bone: 13500–14000MPa,
» ischium and pubis: 14000-14500 MPa.

Cancellous bone was also divided into a couple of part:

Ξ external layer of bone (2000-2600 MPa):
  » surroundings of acetabulum,
  » upper and lower part of bone,
Ξ internal layer of bone:
  » surroundings of acetabulum: 250–300 MPa,
  » upper and lower part of bone: 200–250 MPa.

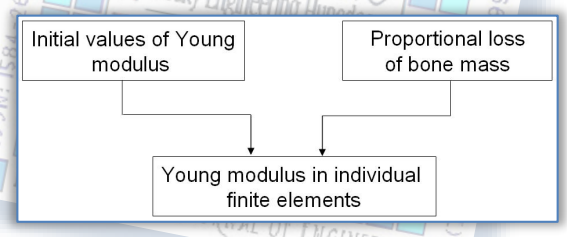

Figure 16. Determining of elastic modulus in individual finite element

In each of these groups values of elastic modulus in individual finite element was determined on the base of decreasing of bone mass and the range of changeability of Young modulus (Figure16). During calculations following relationship was used:

- for cortical bone – conception of Weinans [24]:

$$E = 4.249 \cdot \rho^3 \tag{6}$$

- for cancellous bone – conception of Mow and Hayes [24]:

$$E = 2.195 \cdot \rho^3 \tag{7}$$

where: E – elastic modulus, ρ – radiological density of bone tissue.

It is possible to change these formulas to another and computation distribution of material properties according to different relationships. Some results of numerical simulations are put into Table 3 and Table 4.

Table 3. Displacements and stresses for loss of bone mass in upper part of ilium ala

loss of bone mass [%]	u_{max} [mm]	σ_{max} [MPa]
0	1,38	157
10	1,51	149
20	1,68	140
30	1,89	144
40	2,16	154
50	2,49	164

Table 4. Quantities for loss of mass in pubic symphysis and joint of pelvic and sacral bone

loss of bone mass [%]	u_{max} [mm]	σ_{max} [MPa]	ε_{max}
0	1,38	157	$8{,}00 \cdot 10^{-3}$
10	1,49	148	$1{,}14 \cdot 10^{-2}$
20	1,62	137	$1{,}50 \cdot 10^{-2}$
30	1,79	130	$2{,}00 \cdot 10^{-2}$
40	1,98	144	$2{,}70 \cdot 10^{-2}$
50	2,22	162	$3{,}67 \cdot 10^{-2}$

After building the numerical model the next step of work is to develop procedure to aid of recognizing osteoporotical changes in pelvic bone. The general principle is as follow: after radiology examination it takes place searching to finding the most similar images (searching CT photo from data base). When these images are found the whole model with strength parameters is assigned. Next the results (from strength calculations) are analyzed. As a consequence, particular images from QCT are subordinated effort of bone. In case of need it is possible to return to searching of base and analyzing the larger number of data. The simplified block diagram of the program is presented on Figure 17.

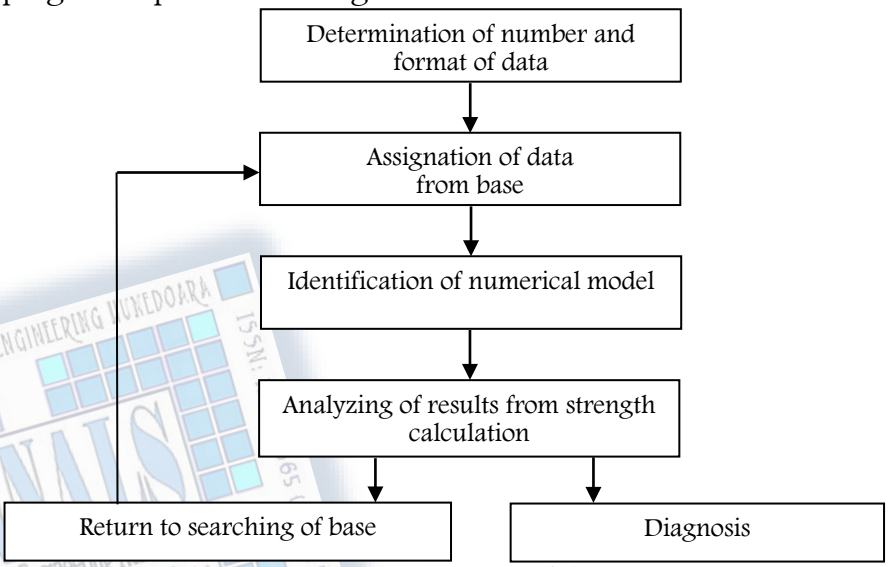

Figure 17. The block schema of the program

In the program there are available two searching procedures: on the base of tomography images and decreasing of bone mass. In procedure of searching on the basis of QCT, one have to first read image – which will be analyzed, next to read images from data base. When sorting is ready, one should to insert number of image, which is the most similar, to the textbox of the program – the information about dangerous state will appear in the window of the program (Figure 18a).

In procedure of searching on the basis of loss of bone mass one should indicate the proportional decreasing of bone mass (from the combo box) in each subregions of cortical bone in numerical model of pelvic bone. When all list are ready in the window of the program will appear information about dangerous state and potential dangerous of osteoporosis (Figure 18b).

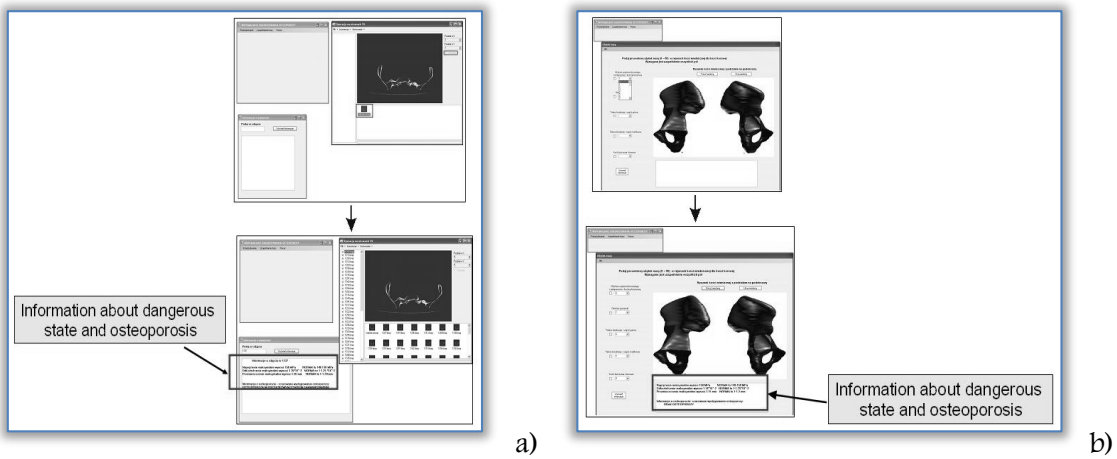

a) b)

Figure 18. Algorithm of the searching on the base of QCT images (a) and on the base of loss of bone mass (b)

On base of obtained results the following conclusion can be prescribed:

» Applied procedure facilitates interpretation the data from QCT and it helps diagnosis what enable earlier detection of osteoporosis and enlarges chance of the treatment.
» Presented procedure delivers additional information about effort state in analyzed bone.
» Information from QCT can be helpful for researching progress of osteoporosis in individual clinical cases (because easier one can find the differences between earlier and later images).
» Subordinating individual images from QCT of effort state provides information about bone system.
» Creation of numerical model on the base of radiological data (especially material properties) increasing its conformance to real conditions.
» Quality of obtained results depends on amount information gathered in the data base.
» Presented procedure enables noticing changes in bones more precisely than standard methods (this is important when the difficulties with clear diagnosis appear).
» Structure of data base enables easy and quick extension.

4. CONCLUSIONS

Combination of numerical simulation and experimental research is needed to obtain correct results and broaden the spectrum of relevant parameters necessary to support surgical and rehabilitation. Both approaches require modern equipment and advanced testing methods. Based on the survey conclusions can be formulated as follows.

» Advanced methods allow to measure the displacement and strain on biological specimens. Here, the MTS universal testing machine (MTS Insigth 10 kN) connected with the Digital Image Correlation system (Dantec Dynamics) were used.
» Obtained results allow to compare the displacement and strain from experiment and numerical simulation. The comparison indicates a good agreement between them.
» Generally, in experiment we can observed selected results (displacement and strain using DIC) on the external surface of sample. On the base of displacement and strain we can calculate the stresses after assuming material parameters. From numerical simulation, after FEM analysis we obtained full set of mechanical parameters useful in planning of surgical intervention (THA, pelvis reconstruction), aided the diagnostic in risky state and design of prosthesis.
» Only the numerical model verified in experiment can be used in computer aided of medical interventions. In this work numerical models were verified and obtained resulst may provide a basis for future research.

REFERENCES

[1.] An Y.H., Draughn R.A.: Mechanical testing of bone and the bone–implant interface. CRC Press, Boca Raton, USA 2000.
[2.] Feng L., Jasiuk I.: Effect of specimen geometry on tensile strength of cortical bone. Journal of Biomedical Materials Research, Vol. 95a(2), 2010, pp. 580-587.
[3.] Keaveny T.M., Pinilla T.P., Crawford R.P., Kopperdahl D.L., Lou A.: Systematic and random errors in compression testing of trabecular bone. Journal of Orthopeadic Research, Vol. 15 (1), 1997, pp. 101-106.

[4.] Keyak J.H., Kaneko T.S., Tehranzadeh J., Skinner H.B., Predicting proximal femoral strength using structural engineering models. Clin. Orthop. Relat. Res., 2005, pp.2 19-228.
[5.] Tanck E., van Aken J.B., van der Linden Y.M., Schreuder H.W., Binkowski M., Huizenga H., Verdonschot N., Pathological fracture prediction in patients with metastatic lesions can be improved with quantitative computed tomography based computer models. Bone 2009;45, pp. 777-783.
[6.] Kokot G., Binkowski M., John A., Gzik-Zroska B.: Advanced mechanical testing methods in determining bone material. Mechanika: Proccedings of 17th International Conference, Kaunas 2012, pp. 139-143.
[7.] Olivier W.C., Pharr G.M., An improved technique for determining hardness and elastic-modulus using load and displacement sensing indentation experiments, Journal of Materials Research, 7(6), 1992, pp. 1564-1583.
[8.] John A., Kokot G., Duda M., Preliminary analysis of the human hip physiologically correct and after surgery resurfacing. Current problems of biomechanics. Scientific Papers of the Department of Applied Mechanics, No. 4, pp. 79-85, Gliwice 2010, (in Polish).
[9.] John A., Identification and analysis of geometrical and mechanical parameters of human pelvic bone, Scientific Papers of Silesian University of Technology, No. 147, Gliwice 2004, (in Polish).
[10.] Rho J.Y., Hobatho M.C., Ashman R.B. Relations of mechanical properties to density and CT number in human bone. Medical Engineering & Physics, 1995, Vol. 17 p. 347-355.
[11.] Dąbrowska-Tkaczyk A., Experimental investigations and computer simulations in human joint arthoplasty. Material from Workshops, International Conference of the Polish Society of Biomechanics, Biomechanics 2010, pp. 33-45, Warsaw 2010.
[12.] Hung-Wen W., Shih-Sheng S., Shyh-Hua E.J., Chiuan-Ren Y., Cheng-Kung C., The influence of mechanical properties of subchondral plate, femoral head and neck on dynamic stress distribution of the articular cartilage. Medical Engineering & Physics, 27 (2005), pp. 295–304.
[13.] De´marteau O., Pillet L., Inaebnit A., Borens O., Quinn T.M., Biomechanical characterization and in vitro mechanical injury of elderly human femoral head cartilage: comparison to adult bovine humeral head cartilage. OsteoArthritis and Cartilage (2006) 14, pp. 589 – 596.
[14.] Thompson M. S., The design of a novel hip resurfacing prosthesis, Thesis submitted for the degree of Doctor of Philosophy, Interdisciplinary Research Centre in Biomedical Materials, Queen Mary and Westfield Collage , University of London; Unit for Joint Reconstruction, Institute of Orthopedics, Robert Jones and Agnes Hunt Orthopedic Hospital, Oswestry 2001.
[15.] McNamara, L.M., Prendergast P.J., Schaffler M.B. Bone tissue material properties are altered during osteoporosis. Musculoskeletal Neuronal Interact, vol. 5, pp.342-343, 2005.
[16.] Pruszyński, B. Radiology: pictorial diagnostics. PZWL, Warszawa 2005 (in Polish).
[17.] Webb, W.R., Brant W.E., Schaffler, M.B. Fundamentals of Body CT. Elsevier Urban & Partner, Wrocław 2007 (in Polish).
[18.] Zagrobelny, Z., Woźniewski M. Clinical biomechanic. AWF Wrocław, 1999 (in Polish).
[19.] Binkowski, M., Dyszkiewicz A., Wróbel Z. The analysis of densitometry image of bone tissue based on computer simulation of X-ray radiation propagation through plate model. Comput. Biol. Med., vol. 37, pp. 245-250, 2006.
[20.] Lee, D. The pelvic Girdle. DB Publishing, Warszawa 2001 (in Polish).
[21.] Rho J. Y., Hobatho, M.C., Ashman R.B. Relations of mechanical properties to density and CT number in human bone bone, Medical Engineering & Physics, vol. 17, pp. 347-355, 1995.
[22.] Dąbrowska-Tkaczyk, A., Domański, J., Lindemann, Z., Pawlikowski, M., Skalski, K. Stress and strain distributions in the bones of hip joint assuming non-homogenous bone material properties. Proc. of II Int. Conf. on Computational Bioengineering 2005, vol. 2, pp. 263-275.
[23.] Gregory, J.S., Aspden, R.M. Femoral geometry as a risk factor for osteoporotic hip fracture in men and women, Medical Engineering &Physics, vol. 30, pp. 1275-1286, 2008.
[24.] Cowin S. C. (Ed.), Bone mechanics handbook, CRC Press LLC, 2001.

ANNALS of Faculty Engineering Hunedoara
– International Journal of Engineering